

# Automatic identification of whiteflies, aphids and thrips in greenhouse based on image analysis

Jongman Cho, Junghyeon Choi, Mu Qiao, Chang-woo Ji, Hwang-young Kim, Ki-baik Uhm, and  
Tae-soo Chon

**Abstract**—Automatic identification of the selected pest insects in greenhouse, whiteflies, aphids, and thrips, was carried out on the specimens collected on yellow sticky traps. Algorithms for image processing were proposed, implemented and tested in this study. Various morphological features of specimens were extracted and analyzed. The size and color components of object were selected as the features for automatic identification. Aphids were easy to discriminate because they have small variation in color information and the body size is substantially different from other species. Identification error was reduced when the data for thrips and whiteflies were analyzed after the aphids were recognized. The reference values of size and color components sampled from 50 insects for each species were accordingly used to characterize the species and methods.

**Keywords**—Aphids, Automatic Identification, Image Processing Techniques, Thrips, Whiteflies

## I. INTRODUCTION

MINIMAL use in pesticides is desired in pest control to cope with various problems caused by over-use of pesticides: acute toxicity to humans and animals, pest resistance to pesticides, change in pest status in agro-ecosystems, high cost of control practices, residue problems in environment, etc [1]. In order to achieve maximal effects of pest control in minimal use of pesticides, accurate estimation of pest densities in field condition is a prerequisite. Based on accurate information on

pests, the most suitable pest management strategies could be designed.

Conventionally, identification and counting of insect specimens have been mostly relied on visual judgment by humans. Consequently, the data obtained by visual judgment for pest densities were less accurate because of the different levels of identification skills and fatigues in continuous sampling and it requires long time for counting a large number of insects on the yellow sticky traps. Automatic detecting system is desired for objective estimation of a large number of pest insects in a short time period.

Considering that economic importance of crops and strong impacts of damage levels as well, pest insects in greenhouse were selected as target species for detection in this study. Whiteflies, aphids and thrips are well-known harmful insects causing severe damage in greenhouse crops in the world [2]. Consequently, management of greenhouse insect pest is one of the main issues in current agricultural practices.

The image processing system has been used for detecting various biological organisms including micro-organisms and plants [3]-[5]. However, relatively few studies have been reported on insects. Honey bees and wasps have been automatically detected based on morphological characteristics, wing venation [6], [7]. Recently, specimens of rice plant hopper on rice paddy fields have been detected by using digital image processing system [8].

This paper extends implementation of the image processing algorithms and techniques to insect pests in greenhouse. By establishing an automated identification system for estimating pest densities in densely populated conditions in greenhouse, the minimization of pesticide application and efficient pest management strategies could be established. Only the three kinds of insect pests, whitefly, aphid and thrips were studied in this study to test the feasibility of the system.

## II. MATERIALS AND METHODS

### A. Collection of Specimens

The experiments on identification were carried out in our laboratory. The specimens of whiteflies, aphids and thrips were collected in the laboratory of Entomology Division, National Institute of Agricultural Science and Technology, Rural Development Administration, Korea. The specimens were collected on the sticky traps in the laboratory conditions, and were used for developing and testing the image processing system. Fig.1 shows a typical yellow sticky trap which is used

Manuscript received February 27, 2007; revised March 27, 2007

Jongman Cho is with the Department of Biomedical Engineering, Inje University, Gimhae, 621-749 Republic of Korea (phone: +82-55-320-3293; fax: +82-55-327-3292; e-mail: injebme@gmail.com).

Junghyeon Choi is with the Department of Biomedical Engineering, Inje University, Gimhae, 621-749 Republic of Korea (e-mail: cjh0713@gmail.com).

Mu Qiao is with the Department of Biological Science, Pusan National University, Busan, 609-735 Republic of Korea (e-mail: allassea@hanmail.net).

Chang-woo Ji is with the Department of Biological Science, Pusan National University, Busan, 609-735 Republic of Korea (e-mail: wittman58@empal.com).

Hwang-young Kim is with the Entomology Division, National Institute of Agricultural Science and Technology, Rural Development Administration of Korea, Suwon, 441-707 Republic of Korea (e-mail: kim3@rda.go.kr).

Ki-baik Uhm is with the Entomology Division, National Institute of Agricultural Science and Technology, Rural Development Administration of Korea, Suwon, 441-707, Republic of Korea (cjh99@bse.inje.ac.kr)

Tae-soo Chon is with the Department of Biological Science, Pusan National University, Busan, 609-735 Republic of Korea (e-mail: tschon@pusan.ac.kr).

in green houses and we used the same sticky traps in this study. The sticky trap is 100 mm wide and 150 mm long in size and its sticky surface area is divided by thick green solid and dotted lines for easy manual identification and counting process. We put the conventional sticky trap on the concave frame made of paper hardboard to provide 1 mm gap between the surface of the sticky trap and the surface of the glass panel of the scanner while the sticky trap is being scanned. Fig. 2 shows a part of a sticky trap which has three kinds of insects under study. Ten sticky traps were prepared for the study.

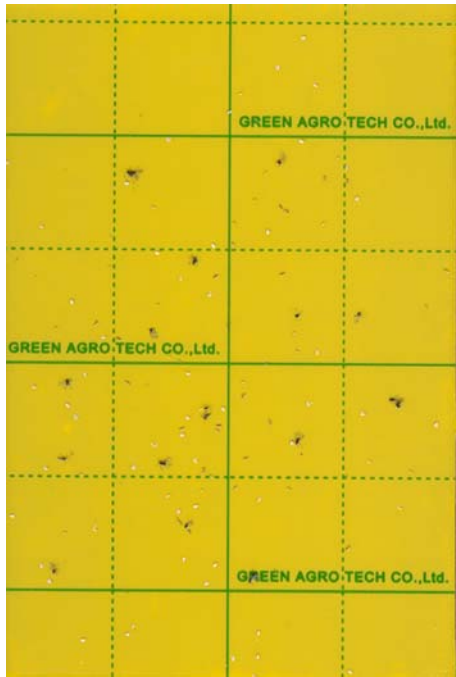


Fig. 1 A typical yellow sticky trap used in this study. It is 100 mm wide and 150 mm long in size and its sticky surface area is divided by thick green solid and dotted lines for easy manual identification and counting process.



Fig. 2 The partial view of a sticky trap on which three kinds of insects under study are trapped.

Each sticky trap was scanned in different spatial resolutions – 200, 300, 600, 1200, and 2400 dots per inch (dpi) and 24-bit per pixel in color depth by flatbed scanner (HP Scanjet

G3010®) to determine the optimal spatial resolution of the scanned image for the identification and each scanned image file was saved as a uncompressed lossless bitmap file format not to lose any information contained in the scanned image. Identification errors decreased for the higher spatial resolution images, but it took very long time for scanning and processing and a large capacity of computer memory so that it was not practical for the images which have the spatial resolution of 1200 dpi or higher as described in Table I. The spatial resolution of 600 dpi was selected as an optimal resolution for

TABLE I  
THE SIZE OF IMAGE FILE FOR DIFFERENT SPATIAL RESOLUTIONS

Spatial resolution	Size of an image file (kByte)
200 dpi	2,658
300 dpi	5,982
600 dpi	23,926
1,200 dpi	95,704
2,400 dpi	382,813

this study.

### B. Image Processing

The dominant color component of the background of the sticky trap used in this study was mainly yellow – average value of red component was 220/255, green was 190/255 and blue was 20/255, where the number 255 in denominator means its maximum value.

Three kinds of typical features including size, morphological feature (shape of boundary), and color components were considered and investigated to identify the three kinds of adult insects, whiteflies, aphids and thrips, and their average values for these features are showed in Table II. Each value indicates the average value for the 50 adult insects.

The information for the size and color components could be common features for the same kind of insects, but morphological boundary feature could not be used as common feature because the attached part of each insect was different depend on the cases. As a result, only the size and three color components showed in Table II were used in this study for

TABLE II  
THE AVERAGE VALUE FOR THE TYPICAL FEATURES USED TO IDENTIFY THE THREE KINDS OF ADULT INSECTS, WHITEFLIES, APHIDS AND THRIPS.

Features	Whiteflies	Thrips	Aphids
<i>Size of adult insects</i> (average number of pixels in the 600 dpi image)	346	246	244
<i>Red color component</i> (maximum value is 255)	228	195	80
<i>Green color component</i> (maximum value is 255)	214	163	67
<i>Blue color component</i> (maximum value is 255)	176	90	47
<i>Morphological features</i> (Shape of boundary)	No common value exists		

identification.

Aphids were easy to discriminate because they have small variation in color information and the body size is substantially different from other species. So, aphids were identified and extracted first and the other two insects were identified later to decrease classification error.

### C. Identification of Aphids

A body part of an aphid has its typical color information which is definitely different from that of other two kinds of insects in the scanned image. The color components of wings of an aphid could not be used because they are very similar to those of other two kinds of insects or background color. Therefore, only the body part image of an aphid was extracted and the information of color and size for this part was used to identify an aphid.

First, the scanned 24-bit color image was converted into 8-bit gray level image for the fast processing. The body part of an aphid appears black color as shown in Table II, so it takes less processing time to extract the body part of aphid from gray scale image rather than from the 24-bit color image. Equation (1) was used for this conversion [9] and Fig. 3 depicts the 8-bit gray level image converted from the 24-bit color image shown in Fig. 2.

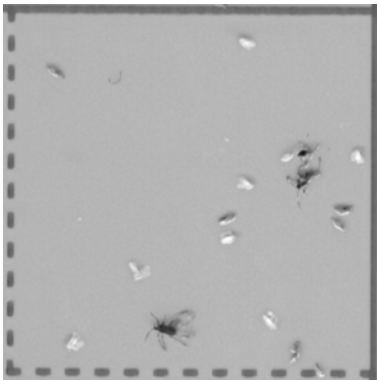


Fig. 3 The 8-bit gray level image converted from 24-bit color image shown in Fig. 2.

In (1),  $f_{gray}$  denotes converted gray level,  $f_{red}$ ,  $f_{green}$ , and  $f_{blue}$  denote red, blue, and green color component respectively.

$$f_{gray} = 0.299f_{red} + 0.587f_{green} + 0.114f_{blue} \quad (1)$$

The aphid objects in this gray scale image appear dark color and other insects appear bright color. If the intensity value of each pixel in this 8-bit gray level image is inverted, the aphids appear bright objects, which makes it easier to extract aphid objects from the image by removing one big dark object including background in the inverted image. Fig. 4 shows the inverted image of the image shown in Fig. 3.

The inverted 8-bit gray level image was converted into the binary image as shown in Fig. 5 to discriminate the body part of aphid from the background image by applying the threshold

level which was determined using the brightness information of all pixels contained in the inverted 8-bit gray level image.

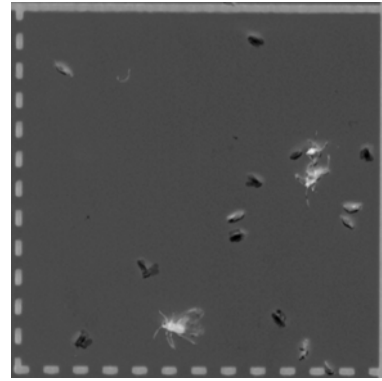


Fig. 4 The inverted 8-bit gray level image of the image shown in Fig. 3. Aphids appear bright color and other objects and background appear dark color.

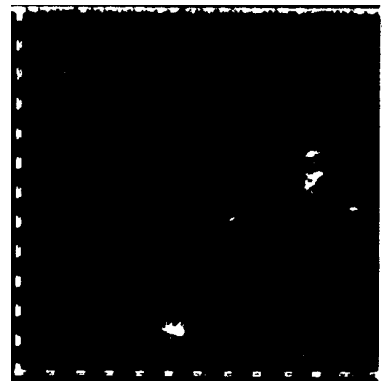


Fig. 5 Binary image obtained from the image shown in Fig. 4. Only the body parts of aphids appear in white color.

The proper threshold level should be determined to get the optimized binary image from the 8-gray level image and many algorithms which calculate the proper threshold level have been developed. The algorithm that determines the threshold level using the iterative method was used in this study [10], [11].

**Step 1.** Select an arbitrary initial threshold level  $T_k$

**Step 2.** Calculate  $\mu_{k1}$ , the average intensity level for the pixels

which have lower intensity level than  $T_k$  and  $\mu_{k2}$ , the average intensity level for the pixels which have higher intensity level than  $T_k$ . The new threshold  $T_{k+1}$  is obtained by (2), and  $\mu_{k1}$  and  $\mu_{k2}$  are determined by (3).

$$T_{k+1} = \frac{(\mu_{k1} + \mu_{k2})}{2} \quad (2)$$

$$\mu_{k1} = \frac{\sum_{i=0}^{T_k} i \cdot h[i]}{\sum_{i=0}^{T_k} h[i]}, \quad \mu_{k2} = \frac{\sum_{i=T_k+1}^{255} i \cdot h[i]}{\sum_{i=T_k+1}^{255} h[i]} \quad (3)$$

In (3)  $h[i]$  is the normalized histogram value for the intensity level of  $i$ . Therefore, the  $T_{k+1}$  can be obtained by (4).

$$T_{k+1} = \frac{1}{2} \left( \frac{\sum_{i=0}^{T_k} i \cdot h[i]}{\sum_{i=0}^{T_k} h[i]} + \frac{\sum_{i=T_k+1}^{255} i \cdot h[i]}{\sum_{i=T_k+1}^{255} h[i]} \right) \quad (4)$$

**Step 3.** Repeat the step 2 until  $T_{k+1}$  does not change.

Once the threshold level  $T$  for the 8-bit gray level image was determined, the new intensity level for the each pixel  $f_2(x, y)$  in the binary image binary can be obtained from the intensity level of the each pixel  $f_{256}(x, y)$  in the 8-bit gray level image by thresholding (5). The  $x$  and  $y$  denote the coordinate of each pixel in the image.

$f(x-1, y-1)$	$f(x, y-1)$	$f(x+1, y-1)$
$f(x-1, y)$	$f(x, y)$	$f(x+1, y)$
$f(x-1, y+1)$	$f(x, y+1)$	$f(x+1, y+1)$

Fig. 6 The four-neighborhood connectivity.

$$f_2(x, y) = \begin{cases} 0 & \text{if } f_{256}(x, y) \leq T \\ 255 & \text{if } f_{256}(x, y) > T \end{cases} \quad (5)$$

All of the white color objects in the binary image are segmented and labeled [9], [12], [13] after thresholding.

We used four-neighborhood connectivity in the labeling process as described following. In Fig. 6, only four pixels,  $f(x, y-1)$ ,  $f(x-1, y)$ ,  $f(x+1, y)$ , and  $f(x, y+1)$  are considered to be connected to the pixel  $f(x, y)$ .

The scanning process runs from the top line of the image to the bottom and from the leftmost pixel in the line to the rightmost pixel. Therefore, the two neighborhood pixels,  $f(x, y-1)$  and  $f(x-1, y)$ , were already scanned when the pixel  $f(x, y)$  is scanned if the pixel  $f(x, y)$  is not on the boundary of the image. The labeling of the pixel  $f(x, y)$  is dependent on the following four conditions of the two neighbor pixels which were already scanned.

**Case 1.** If none of two neighborhood pixels were labeled, a new label is assigned to the pixel.

**Case 2.** If only one pixel was labeled, the same label is assigned to the pixel.

**Case 3.** If both of the two neighborhood pixels were labeled with the same number, the same label is assigned to the pixel.

**Case 4.** If the two pixels were labeled with different numbers, the smaller labeling number is assigned to the pixel and the same smaller labeling number is assigned to the pixel which has the larger labeling number.

Therefore, all the pixels which have the same labeling number can be considered to be one object. If the size, i.e. the number of pixels of an object is in the predetermined range obtained from 50 aphids in the previous experiment, the object is selected as a candidate of an aphid and its original color information is restored from the 24-bit color image as shown in Fig. 7. Each object which has the size out of the predetermined range is excluded automatically in this process.



Fig. 7 Color information for the selected objects was restored from the 24-bit color image.

As shown in Fig. 5 and Fig. 7, many dots which are parts of dotted lines and parts of other insects are also selected as candidates for aphids if the size of them is in the predetermined range. These noise objects can be excluded in the following filtering process based on their color components.

If the color information, i.e. the average color intensity values for red, green, and blue color components for each aphid candidate is in the predetermined range obtained from 50 aphids in the previous experiment, the object is finally selected as an aphid and it is marked with a small cross in the original 24-bit color image to show that it was identified as an aphid as shown in Fig. 8. Though the size of each object is in the predetermined range of aphids, the object which has the color components out of the predetermined range is excluded automatically in this process.

#### D. Identification of Whiteflies and Thrips

It causes identification errors when whitefly or thrips is

touched by an aphid. To avoid this problem, each identified aphid and green colored grid marks are erased by overwriting them with the background color in the 24-bit color image [6] and we can get an intermediate image as shown in Fig. 9.

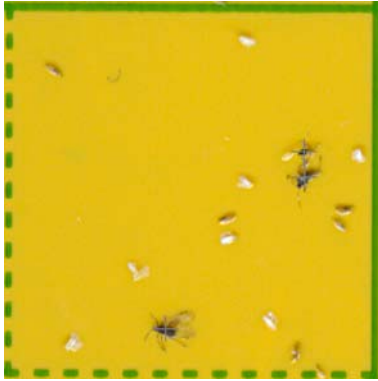


Fig. 8 All objects which were identified as aphids were marked with a small cross to show the identification result.

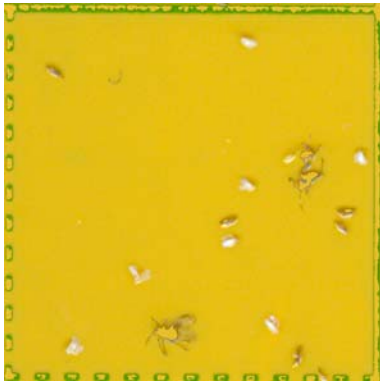


Fig. 9 Identified aphids and grid marks were erased by overwriting them with the background color.

Whitefly and thrips have similar size information but different color information in the intermediate image. However, their boundaries have similar color information with the background color in the intermediate image and this causes errors during segmentation process of these types of insects. The YUV color image model can be used to extract more accurate boundary of the object which is placed in similar background color and the intermediate image which has red ( $R$ ), green ( $G$ ), and blue ( $B$ ) color components is converted into YUV format using (6) [10].

$$\begin{aligned} Y &= 0.3R + 0.59G + 0.11B \\ U &= 0.493(B - Y) \\ V &= 0.877(R - Y) \end{aligned} \quad (6)$$

Each image for  $Y$ ,  $U$ , and  $V$  component is 8-bit gray level image. The Prewitt edge detection method was applied to  $Y$ ,  $U$ , and  $V$  component image respectively to enhance the boundary information and the edge information for brightness ( $Y$ ) and

two color components,  $U$  and  $V$ , can be obtained separately. An integrated edge enhanced image as shown in Fig. 10 can be obtained by combining the three edge enhanced images for  $Y$ ,  $U$ , and  $V$  component using Euclidean distance (7) [10].

$$D = \sqrt{E_Y^2 + (0.5E_U)^2 + (0.5E_V)^2} \quad (7)$$

In (7),  $D$  denotes combined pixel value in the integrated edge enhanced image and  $E_Y$ ,  $E_U$ , and  $E_V$  mean pixel values in the  $Y$ ,  $U$ , and  $V$  component images respectively.

Each pixel value in the integrated edge enhanced image was multiplied by two to enhance edge component which has low contrast to the background and we could get an edge contrast enhanced image as shown in Fig. 11.

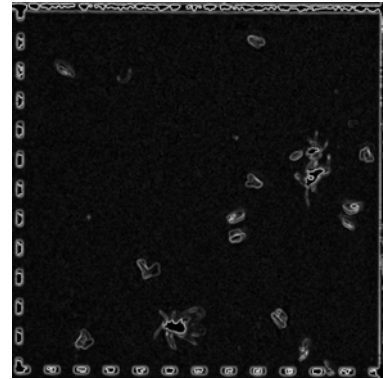


Fig. 10 An integrated edge enhanced image obtained by combining three edge enhanced image of  $Y$ ,  $U$  and  $V$  components.

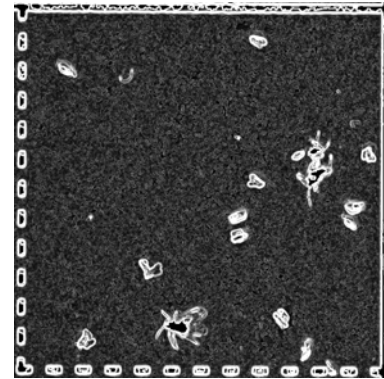


Fig. 11 An edge contrast enhanced image.

The edge contrast enhanced image was converted into binary image to get clear edge information as shown in Fig. 12 and the threshold level was determined by the same method which was used for aphid identification.

Each object in the binary edge image has edge information but no information for the internal area, and this information for the internal area is necessary for correct segmentation and labeling processes followed. All the pixels in the external area of each edge detected object are connected and can be considered as one big object. The internal area of each object

can be obtained by extracting and removing this big external object from the image. The internal area of each object is filled up with the pixel value of the boundary gray level and we can obtain a new image in which the internal area of each object is filled up as shown in Fig. 13.

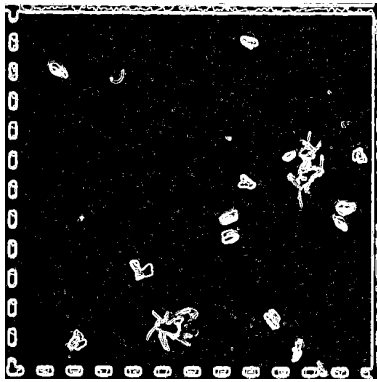


Fig. 12 A binary edge image showing clear edge information was obtained by binary conversion with threshold level. An edge contrast enhanced image.



Fig. 13 The internal area of each object is filled up.

However, some objects in this image are connected to other objects or grid marks and this causes errors in counting objects. This problem can be solved by applying two times of erosion processing and we can get an image in which the connected objects are separated as shown in Fig. 14.

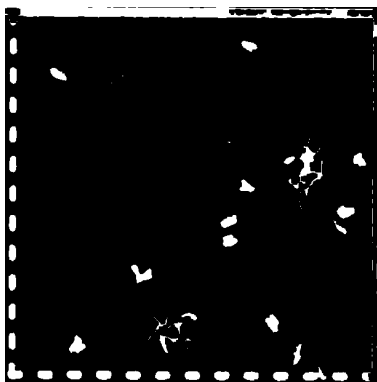


Fig. 14 Connection to other objects could be removed by applying two times of erosion processing. The internal area of each object is filled up.

The next processing procedures, segmentation and labeling, are the same as those of aphid identification. If the size, i.e. the number of pixels of an object is in the predetermined range, the object is selected as a candidate of a whitefly or thrips respectively and its original color information is restored from the 24-bit color image as shown in Fig. 15. Each object which has the size out of the predetermined range is excluded automatically in this process.



Fig. 15 The color information of each object was restored.

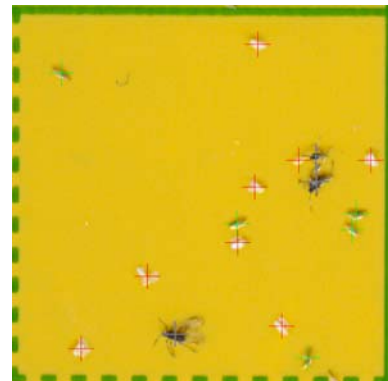


Fig. 16 Identification of three kinds of target insects.

If the color information, i.e. the average color intensity values for red, green, and blue color components for each whitefly or thrips candidate is in the predetermined range obtained from 50 whiteflies and thrips in the previous experiment, the candidate is finally selected as a whitefly or thrips respectively and it is marked with a small cross in the original 24-bit color image to show that it was identified as a whitefly or thrips as shown in Fig. 16 where whiteflies, thrips, and aphids are marked with a red, green, and complementary colored cross respectively. Though the size of each object is in the predetermined range of whitefly or thrips, the object which has the color components out of the predetermined range is

excluded automatically in this process.

Finally, the selected aphids, whiteflies, and thrips are counted and the number of each species is reported.

### III. RESULTS

#### A. Determining the Reference Value

The range of the body size and the value of the three color components, red, green, and blue, of aphids, whiteflies, and thrips were investigated for the 50 adults respectively by manual processing and Table III shows the results. Each of

TABLE III  
REFERENCE VALUES USED FOR IDENTIFICATION PROCESS WERE DETERMINED BY  
EXPERIMENTS FOR 50 OBJECTS OF APHIDS, WHITEFLIES AND THRIPS

Color and Size	Whiteflies				Thrips				Aphids			
	R	G	B	Size	R	G	B	Size	R	G	B	Size
Minimum	214	201	145	225	176	142	50	144	50	41	28	77
Average	228	214	176	346	195	163	90	251	80	67	47	244
Maximum	240	227	195	449	214	186	124	452	119	96	57	540

these values was used as a reference in the identification process of the three insects. The body size of the insect in the Table III indicates the number of pixels in the 600 dpi scanned image and the maximum value of each color component is 255 in the 24-bit color image.

#### B. Identification Results

TABLE IV  
IDENTIFICATION RESULT

Image	Recognition by expert			Recognition by system			Accuracy (%)		
	Whitefly	Aphid	Thrips	Whitefly	Aphid	Thrips	Whitefly	Aphid	Thrips
1	30	0	27	22	0	18	73.3	100	66
2	32	0	40	29	0	37	90.6	100	92
3	5	18	24	5	16	20	100	88.8	83
4	53	17	25	51	16	25	96.2	94.1	100
5	136	22	33	120	13	33	88.2	59.1	100
6	46	12	32	42	13	31	91.3	91.6	96
7	1	0	48	1	0	40	100	100	83
8	1	16	20	1	15	23	100	93.7	85
9	1	0	58	1	0	53	100	100	91
10	0	1	43	0	1	40	100	100	93

The proposed image processing and identification algorithms were applied to the ten scanned images of the sticky traps, which were not used in the process of the determining of the reference values. Finally, we obtained the identification result as shown in Table IV.

### IV. CONCLUSION

It was easy to discriminate aphids from other two insects because aphids showed small variation in color information and the size of aphids is very different from that of the other two

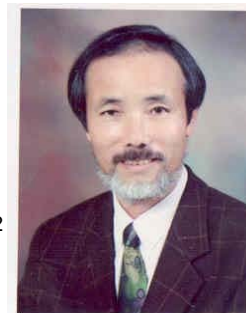
kinds of insects. Aphid was identified by extraction of its body part only and its wing parts were discarded because they did not have common morphological shapes when an aphid is stuck to a sticky trap and their color components also have huge variation. Thrips and whiteflies were identified based on their sizes and color components after aphids were identified and removed to reduce identification error.

The reference values of size and color components for the identification processes were predetermined before the identification of target insects through the experiments for 50 adult insects respectively.

The color components of sticky trap used in this study were similar to those of thrips, which caused identification error. In addition, the green colored grid marks printed on the sticky trap also caused identification error. The identification error will decrease if we design a new sticky trap without grid marks which has different color components from those of the three kinds of insects.

### REFERENCES

- [1] G. T. Miller, *Sustaining the Earth*, Thompson Learning, Inc., Pacific Grove, California, 2004, pp. 211-216.
- [2] M. Malais, and W. J. Ravensburg, *Knowing and Recognizing: The biology of glasshouse pests and their natural enemies*, Koppert Biological Systems, pp. 109.
- [3] D. Dörge, J. M. Carstensen and J. C. Frisvad, "Direct identification of pure *Penicillium* species using image analysis," *Journal of Microbiological Methods*, vol. 41, pp. 121-133, 2000.
- [4] Y. P. Ginoris, A. L. Amaral, A. Nicolau, M. A. Z. Coelho and E. C. Ferreira, "Recognition of protozoa and metazoan using image analysis tools, discriminant analysis, neural networks and decision trees," *Analytica Chimica Acta*, vol. 595, pp. 160-169.
- [5] J. C. Neto, G. E. Meyer, D. D. Jones and A. K. Samal, "Plant species identification using Elliptic Fourier leaf shape analysis," *Computer and Electronics in Agriculture*, vol. 50, pp. 121-134.
- [6] S. W. T. Batra, "Automatic image analysis for the rapid identification of Africanized honey bees," *In Africanized Honey Bees and Bee Mites*, eds, Needham, G. H., Page R. E., Delfinado-Baker, M., and Bowman, C. E., Ellis Horwood, Chichester, U. K., 1988, pp. 260-263.
- [7] A. T. Waston, M. A. O'Neill and I. J. Kitching, "Automated identification of live moths (Macrolepidoptera) using Digital Automated Identification System (DAISY)," *Systematics and Biodiversity*, vol. 1, pp. 287-300.
- [8] Y. S. Park, M. W. Han, H. Y. Kim, K. B. Uhm, C. G. Park, J. M. Lee and T. S. Chon, "Density Estimation of Rice Planthoppers Using Digital Image Processing Algorithm," *Korean J. Appl. Entomol.*, vol. 42, pp. 57-63.
- [9] Gregory A. Baxes, *Digital Image Processing*, Wiley, 1994, pp. 123-152.
- [10] S. K. Hwang, *Image Processing Programming by Visual C++*, Hanbit Media, 2007, pp. 660-671.
- [11] Yun Q. Shi, Huifang Sun, *Image and Video Compression for Multimedia Engineering*, CRC, 2000, pp. 169-175.
- [12] Stephen P. Banks, *Signal Processing Image Processing and Pattern Recognition*, Prentice Hall, 1990, pp. 264-266.
- [13] Dwayne Phillipis, *Image Processing in C*, R&D Technical Books, 1994, pp. 213-220.
- [14] Tzay Y. Young, *Handbook of Pattern Recognition and Image Processing*, Academic Press, 1986, pp. 215-230.



**Jongman Cho** was born in Seoul, Korea, in 1957. He received the B.E., M.E. and Ph.D. degrees in electronic engineering from Inha University, Incheon, Korea in 1985, 1989 and 1994 respectively.

Since 1990 he has been working at the Department of Biomedical Engineering, Inje University, Gimhae, Korea and now he is an

ASSOCIATE PROFESSOR. During 1996- 1998, he stayed at the Department of Biomedical Engineering, Rutgers University, NJ, U.S.A. as a visiting scholar. His research area includes signal processing, application of artificial neural network and telemedicine.

Prof. Cho is a member of IEEE EMBS, IEICE, IEEK, KOSOMBE, and RESKO.